



1 **Effect of wind speed on the size distribution of biogenic gel**
2 **particles in the sea surface microlayer: Insights from a**
3 **wind wave channel experiment**

4

5 **Cui-Ci Sun^{1,2,3}, Martin Sperling¹, Anja Engel¹**

6 [1] GEOMAR Helmholtz Centre for Ocean Research Kiel, 24105Kiel, Germany

7 [2] State Key Laboratory of Tropical Oceanography, South China Sea Institute of
8 Oceanology, Chinese Academy of Sciences, 510301, Guangzhou, China

9 [3] Daya Bay Marine Biology Research Station, Chinese Academy of Sciences, 518000,
10 Shenzhen, China,

11

12 *Correspondence to:* Anja Engel (aengel@geomar.de)

13

14 Running title: Variation of gel particles in the SML as a function of wind speed

15

16

17

18

19

20

21

22 **Key words:** wind speed, biogenic gel particle, size distribution, air-sea interface,

23



1 **Abstract**

2 Biogenic gels particles, such as transparent exopolymer particles (TEP) and Coomassie
3 stainable particles (CSP), are important components in the sea-surface microlayer (SML). The
4 accumulation of gel particles in the SML and their potential implications for gas exchange
5 and emission of primary organic aerosols have generated considerable research interest in
6 recent years. Changes in the particle-size distribution (PSD) can provide important
7 information for the understanding of physical and chemical processes involving gel particles,
8 such as aggregation, degradation or loss. So far, little is known regarding the influence of
9 wind speed on the size distribution of marine gel particles in the surface microlayer. Here, we
10 present results on the effect of different wind speeds on the PSD of TEP and CSP during a
11 wind wave channel experiment in the Aeolotron. Total area of TEP and CSP were
12 exponentially related to wind speed in the SML. At wind speeds $< 6 \text{ ms}^{-1}$, a strong
13 accumulation of TEP and CSP occurred in the SML, decreasing at higher wind speed and
14 becoming depleted above wind speeds of 8 ms^{-1} . Wind speeds $> 8 \text{ ms}^{-1}$ also significantly
15 altered the PSD slope of TEP in the 2-16 μm size range toward smaller size. Changes in
16 spectral slopes at wind speeds $> 8 \text{ ms}^{-1}$ were more pronounced for TEP than for CSP
17 indicating a high aggregation potential for TEP in the SML, potentially enhancing the export
18 of TEP by aggregates settling out of the SML. Our experiment provided evidence for the
19 control of wind speed on the accumulation of biogenic gel particles and their PSD changes,
20 providing a useful insight into particle dynamics and biophysical processes at the interface
21 between air and sea.

22

23

24



1 **1 Introduction**

2 The sea–surface microlayer (SML) is the thin boundary layer (~50-100 μm) between the
3 atmosphere and the ocean. It is central to a range of global biogeochemical and climate-
4 related processes (Cunliffe et al., 2013). Due to the high variability of physical, biological,
5 chemical, and photochemical interactions, SML properties often differ from the underlying
6 waters (ULW). Previous field and laboratory studies have shown that marine organic gels can
7 been riched in the SML, and highlighted the importance of microgels for increasing
8 gelatinous biofilm formation (Galgani et al., 2014; Wurl and Holmes, 2008) and mediating
9 vertical organic matter transport, either up to the atmosphere or down to the deep ocean. To
10 date, mainly two kinds of gel particles have been widely studied in seawater: transparent
11 exopolymer particles (TEP), which include acidic polysaccharides, and Coomassie stainable
12 particles (CSP) that are protein-containing particles and can serve as a nitrogen source for
13 bacteria and other organisms (Alldredge et al., 1993; Cisternas-Novoa et al., 2015; Long and
14 Azam, 1996; Passow, 2002). TEP are sticky and can increase coagulation efficiencies of
15 particles in seawater (Chow et al., 2015; Engel, 2000). TEP thereby can enhance particle
16 aggregation rate in the ocean and therewith influence element cycling, including trace
17 elements (Passow, 2002). Changes in TEP abundance and size distribution in SML might
18 therefore also influence particle dynamics in the water column below. The formation of TEP
19 represents an abiotic pathway of repartitioning dissolved organic carbon into particulate
20 organic carbon (Engel et al., 2004). Compared to TEP, much less is known for processes
21 controlling CSP formation in SML. It has been suggested that CSP and TEP are different
22 particles, because of their distinct spatial and temporal distributions in the ocean (Cisternas-
23 Novoa et al., 2015; Engel and Galgani, 2016). It has also been reported that enrichment in
24 CSP in the microlayer was related to bacterial activity, implying that bacteria may play a



1 pivotal role in mediating processes at the air-sea interface by contributing exudates and
2 proteins released through cell disruption (Galgani and Engel, 2013).

3 Gel particles have been suggested to play an important role in air-sea exchange processes.
4 Previous results showed that gel particles with a polysaccharidic composition ejected by
5 bubble bursting events may act as cloud condensation nuclei (CCN) in low-level clouds
6 regions (Leck and Bigg, 2005; Orellana et al., 2011; Russell et al., 2010). Also proteinaceous
7 gels and amino acids can be enriched in the SML and in sea-spray aerosols (SSA)
8 (Kuznetsova et al., 2005). Since gel particles with fractal scaling provide a relatively large
9 surface to volume ratio, they are assumed to act as a cover at the interface between air and sea,
10 potentially reducing molecular diffusion rates (Engel and Galgani, 2016). Thus, the
11 enrichment of organic matter, including gels, in the SML could modulate the air-sea gas
12 exchange at low and intermediate winds (Calleja et al., 2009; Engel and Galgani, 2015;
13 Mesarchaki et al., 2015; Wurl et al., 2016). The SML is expected to disrupt at higher wind
14 speed, but the threshold wind speed for organic matter enrichment in general, and for specific
15 components in particular, is largely unknown (Liss, 2005). Wind was determined as a
16 principal force that controls accumulation of particulate material in the SML and as the most
17 important variable controlling the air-sea exchange of gas and particles (Frew et al., 2004; Liu
18 and Dickhut, 1998; UNESCO, 1985). Natural slicks often occur at low wind speeds ($<6 \text{ m s}^{-1}$)
19 typically having wider area coverage for longer time in coastal seas compared to the open-
20 ocean (Romano, 1996). Using different SML sampling methods, such as the teflon plate, glass
21 plate and Garret screen (Garrett and Duce, 1980), direct relationships between wind speed and
22 SML thickness have been determined. Yet, the influence of wind on SML thickness is not
23 clear; Liu and Dickhut (1998) observed a decrease with wind speed up to 5 m s^{-1} , while
24 Falkowska (1999) determined an increase up to a wind speed of 8 m s^{-1} , beyond which the
25 thickness of the SML began to decrease. TEP enrichment in the SML has been described to



1 be inversely related to wind speed greater than 5-6 ms⁻¹ (Engel and Galgani, 2016; Wurl et al.,
2 2009; Wurl et al., 2011). One explanation that has been proposed for the reduction of TEP
3 abundance in the SML is that at higher wind speed, aggregation of solid particles with TEP
4 result in aggregates becoming negatively buoyant and sinking out of the SML. For
5 proteinaceous gels, Engel and Galgani (2016) observed that their enrichment was not
6 inversely related to wind speed. Yet, an inverse relationship between the slope of the CSP size
7 distribution in the SML and wind speed was observed, indicating larger CSP in the SML at
8 low wind speed. In addition, the dynamics of gel particles in the SML were also affected by
9 the other mechanisms that depend on the wind and wave conditions. It is proposed that gel
10 particles formation within the SML by bubble scavenging of DOM in the upper water column
11 (Wurl et al., 2011), because more TEP precursors are lifted up the water-column. Moreover,
12 compression and dilatation of the SML due to capillary waves may increase the rate of
13 polymer collision, subsequently facilitating gel aggregation (Carlson, 1983).

14 Particle-size distribution (PSD) is a trait description of gel particles that relates to many
15 important processes. It has been demonstrated that marine heterotrophs feed on gel particles
16 within specific size ranges (Mari and Kiorboe, 1996). Bacterial colonization TEP varies as a
17 function of the size (Mari and Kiorboe, 1996; Passow, 2002). Thus, changes in the size
18 distribution of biogenic gel particles will likely alter food-web structure and dynamics in the
19 ocean and the SML. Gel PSD and its variation with biogeochemical and physical processes
20 generally reflect the information about coagulation, break-up, and dissolution as well as on
21 sources and sinks of gels particles, either moving upward into or sinking out of the SML. In
22 addition, the abundance and size of marine gels in the SML and in subsurface waters may
23 determine their potential fate as CCN in the atmosphere (Orellana et al., 2011). Wurl et al.
24 (2011) provided a conceptual model for the production and fate of TEP in surface waters and
25 the underlying controlling mechanisms. However, due to the lack of observational data, we do



1 not understand well how the PSD of marine gel particles in the SML varies as a function of
2 wind speed and wave action. Knowledge of the characteristics of gel particles such as
3 abundance, total area and PSD in the SML, and how they relate to wind speed may improve
4 our understanding the marine primary organic aerosol-cloud feedback processes and
5 accurately estimate trace gas fluxes from the ocean to the atmosphere. Here, we assess the
6 dynamics of PSD of marine gels particles, i.e. TEP and CSP, in the SML in responses to
7 different wind speeds and bubbling. This study was conducted in 2014 with natural Atlantic
8 seawater at the ‘Aeolotron’ facility in Heidelberg, a large-scale annular wind-wave channel
9 that allows for full control of wind speed.

10

11

12

13

14

15

16

17

18

19



1 **2 Methods**

2 **2.1 Experimental set up**

3 Effects of different wind speeds on the size distribution of organic gel particles in the SML
4 were studied during the Aeolotron experiment from 3rd to 28th November 2014. In total
5 20.000 L of North Atlantic seawater were collected by the research vessel FS Poseidon,
6 including ~14000 L of high salinity water collected at 55 m at 64° 4,90' N 8° 2,03' E and ~
7 8000 L collected at 5 m depth near the Island of Sylt in the German Bight, North Sea. The
8 water was transferred to a clear tank container and transported to the Heidelberg Aeolotron
9 facility. The 'Aeolotron' is the largest annular wind/wave facility in the world with a total
10 height of 2.4 m, and an outer diameter of 10 m. The wind speed was measured by Pitot tube
11 and anemometer. In order to compare the wind speed with measurements in the field and in
12 other facilities, the facility-specific reference wind speed U_{ref} is of little use. Instead, the
13 friction velocity U_* which is separately determined and converted into the value U_{10} as
14 described in Bopp and Jähne (2014). U_{10} is the wind speed which were measured in ten
15 meters height on the open ocean if the same friction velocity U_* as in the Aeolotron is
16 assumed. A total of 7 experiments were conducted, with stepwise increase in wind speeds
17 (equivalent to U_{10}), ranging from 1.371 to over 18.652 ms^{-1} as shown in Figure 1 and Table
18 1. During some of the high wind speed conditions (Table 1), bubbles were generated in
19 addition with a profiO₂ oxygen diffuser hose to simulate strong breaking waves with bubble
20 entrainment and spray formation. About 54 meters of this tubing were installed and were
21 operated with a pressure of around 900 mbar with normal air taken from the air space of the
22 Aeolotron at a flow rate of around 100 L min^{-1} . In addition, on day 5, day 12 and day 23, one
23 wind speed was arranged at about 18 ms^{-1} with and without bubbling for about 2 hour,
24 respectively. Seawater temperature over the course of the experiment was about 21 °C ± 1.



1 For two periods (days 9-16 and 20-26) light was switched on, and provided
2 Photosynthetically Active Photon Flux Density (PFD) at the water surface of about 115-120
3 $\mu\text{mol m}^{-2} \text{s}^{-1}$ over about 20 m of the tank perimeter, and 20 $\mu\text{mol m}^{-2} \text{s}^{-1}$ for the remaining 10
4 m.

5 Temporal changes in hetero- and autotrophic plankton and neuston abundance and in organic
6 matter during the experiment are described in more detail in Engel et al. (2017) and are
7 summarized here only briefly. Heterotrophic microorganisms dominated cell abundance and
8 biomass in the tank during the whole study. Two peaks of bacterial abundance in the SML
9 occurred on day 4 and on day 11, respectively. On day 20, a seed culture of *Emiliana huxleyi*
10 (cell density: $4.6 \times 10^5 \text{ cell ml}^{-1}$) was added followed by a biogenic SML from a previous
11 experiment on day 21.

12 2.2 Sampling

13 SML samples were collected with a glass plate sampler, made of borosilicate glass with
14 dimensions of 500 mm (length) \times 250 mm (width) \times 5 mm (thickness) and with an effective
15 surface area of 2000 cm^2 (considering both sides). For each sample, the glass plate was
16 inserted into the water perpendicular to the surface and withdrawn at a controlled rate of ~ 20
17 cm sec^{-1} . The sample, retained on the glass because of surface tension, was removed by a
18 Teflon wiper, and for each sample the glass plate was dipped and wiped about twenty five
19 times. The exact number of dips and the volume collected were recorded. Samples were
20 collected into acid cleaned (HCl, 10%) and Milli-Q washed glass bottles. Prior to sampling,
21 both glass plate and wiper were rinsed with Milli-Q water, and intensively rinsed with
22 Aeolotron water in order to minimize their contamination with alien material. The first
23 millilitres of SML sample were used to rinse the bottles and then discarded. The bulk water



1 was sampled from the outlet at the middle-lower part of Aeolotron and collected into acid
2 cleaned (HCl, 10%) and Milli-Q washed glass bottles.

3 **2.3 Analytical methods**

4 Total area, particle numbers and equivalent spherical diameter (d_p) of gel particles were
5 determined by microscopy following Engel (2009). For TEP and CSP, 5 to 30 mL were
6 gently filtered (<150 mbar) onto 25mm Nuclepore membrane filters (0.4 μ m pore size,
7 Whatman Ltd.), stained with 1 ml Alcian Blue solution for polysaccharidic gels and 0.5mL
8 Coomassie Brilliant Blue G (CBBG) working solution for proteinaceous gels. The excessive
9 dye was removed by rinsing the filter with Milli-Q water. Blank filters for gel particles were
10 taken using Milli-Q water.

11 Filters were transferred onto Cytoclear © slides and stored at -20 °C until microscopy analysis.
12 For each filters, 30 images were randomly taken at $\times 200$ magnification with a light microscope
13 Zeiss microscope (Zeiss AxioScope A.1). An image-analysis software (Image J, US National
14 Institutes of Health) was used to analyze particle numbers and area.

15 The size-frequency distribution of TEP and CSP gels was described by:

$$16 \quad \frac{dN}{d(d_p)} = k d_p^\delta \quad (1)$$

17 where dN is the number of particles per unit water volume in the size range d_p to $(d_p+d(d_p))$
18 (Mari and Kiorboe, 1996). The factor k is a constant that depends on the total number of
19 particles per volume, and δ ($\delta < 0$) describes the spectral slope of the size distribution. The less
20 negative is δ , the greater is the fraction of larger gels. Both δ and k were derived from
21 regressions of $\log[dN/d(dp)]$ versus $\log[dp]$ over the size range 2–16 μ m ESD. TEP carbon
22 concentration were calculated from the carbon-size relationship: $TEP-C = 0.25 r^{2.55}$ (pg C
23 TEP^{-1}), where $TEP-C$ (pg C) is the carbon content of a given TEP particle with a radius r (μ m)



1 (Mari et al., 2001).

2 On day11, samples taken during wind condition 1 and 2 were contaminated and therefore
3 removed from data analysis.

4 **2.4 Data analysis**

5 Results from the SML samples were compared to those of bulk water and expressed as
6 enrichment factors (EF), defined as:

$$7 \text{ EF} = (C)_{\text{SML}} / (C)_{\text{B}} \quad (2)$$

8 Where (C) is the concentration of a given parameter in the SML or bulk water, respectively
9 (GESAMP, 1995). Enrichment of a component is generally indicated by $\text{EF} > 1$, depletion by
10 $\text{EF} < 1$. Considering the measurement uncertainty of gel particles using microscopic method
11 within 10%, EF values > 1.1 thus represent significant enrichment of gel particle in the SML,
12 while $\text{EF} < 0.9$ is determined to be a depletion. Enrichment or depletion was hence assumed
13 as being not unambiguously determinable for factors between 0.9 and 1.1.

14 Nonparametric statistics (Two Sample-Kolmogorov-Smirnov test) was performed to compare
15 differences of slope of gel particles size distribution between low and moderate wind speeds
16 ($< 8 \text{ ms}^{-1}$) and high wind speeds ($> 8 \text{ ms}^{-1}$). In addition, statistical significance of changes
17 with respect to the slope of gel particles size distribution after adding the seed culture of
18 *E. huxleyi* and the biogenic SML water from a previous experiment was determined with two
19 sample-Kolmogorov-Smirnov test on non-normalized anomalies given the data being normal
20 distributed. Average values are reported with ± 1 standard deviation. Friedman ANOVA test
21 was carried out to evaluate bubble effect on enrichment in gel particles. Statistical
22 significance was accepted for $p < 0.05$. Calculations and statistical tests were conducted using
23 Microsoft Office Excel 2010 and Origin 9.0 (Origin Lab Corporation, USA) software.



1 3 Results

2 3.1 TEP and CSP developments in bulk and microlayer surface

3 The developments of TEP and CSP in bulk and SML are shown in Figure 2. From day 1 to
4 day 15, average abundance and total area of TEP in the SML were $1.56 \pm 1.05 \times 10^8 \text{ L}^{-1}$ and
5 $1.84 \pm 1.39 \times 10^3 \text{ mm}^2 \text{ L}^{-1}$, respectively. TEP abundance in the bulk water increased from the
6 initial $7.93 \pm 0.09 \times 10^7 \text{ L}^{-1}$ on day 2 to $14.60 \pm 1.45 \times 10^7 \text{ L}^{-1}$ on day 15. TEP total area in the
7 bulk water was $0.38 \pm 0.01 \times 10^3 \text{ mm}^2 \text{ L}^{-1}$ initially and increased to the maximum value of 1.42
8 $\pm 0.10 \times 10^3 \text{ mm}^2 \text{ L}^{-1}$ on day 15. After addition of the *E.huxleyi* seed culture and of pre-
9 collected biogenic SML on day 20, TEP re-accumulated in the SML, with $2.15 \pm 0.72 \times 10^8 \text{ L}^{-1}$
10 1 and $2.92 \pm 1.42 \times 10^3 \text{ mm}^2 \text{ L}^{-1}$, respectively.

11 Similar to TEP, CSP abundance and total area in the SML declined gradually between day 1
12 and 12. Here, CSP abundance in the SML decreased from $1.87 \pm 0.37 \times 10^8 \text{ L}^{-1}$ to 0.30 ± 0.16
13 $\times 10^8 \text{ L}^{-1}$ on day 12, and CSP total area dropped from an initial $2.05 \pm 0.27 \times 10^3 \text{ mm}^2 \text{ L}^{-1}$ to
14 $0.156 \pm 0.065 \times 10^3 \text{ mm}^2 \text{ L}^{-1}$. Generally, abundance and total area were less for CSP than for
15 TEP. The peaks of CSP abundance and total area in both SML and bulk water occurred on
16 day 24 corresponding to increasing of Chl*a* in the bulk water.

17

18 3.2 TEP and CSP abundance and total area variations with respect to wind 19 speeds

20 At the start of each wind experiment, the water surface was flat, without visible surface
21 movement. As the wind speed increased, the first capillary waves became visible and started
22 breaking above about $U_{10} = 6 \text{ ms}^{-1}$ ($U_{10} = 6.099 \text{ ms}^{-1}$ on day 22). At this wind speed, TEP



1 abundance in the SML decreased, except for day 15 and day 11, when TEP abundance
2 remained relatively stable or even increased slightly in SML at high wind speed (Fig. 3).
3 Similar to TEP, abundance and total area of CSP decreased with increasing wind speed,
4 excluding day 11 and day 2 (Fig. 4). The exponential decline of TEP and CSP total area in the
5 SML with increasing wind speed can be described by $\ln y = \ln a + bx$ or $y = ae^{bx}$, where x is wind
6 speed, y is gel particle total area, a is a constant depends on the total area of particles per
7 volume under the initial lowest wind speed condition. Exponential functions are the result of
8 constant relative growth or decline; here b is the relative decline speed for the exponential
9 function. A measure of goodness of fit is the coefficient of determination (COD) denoted as r^2
10 ($b_{\text{CSP-Totalarea}} = -0.20 \pm 0.13$, $r^2 = 0.73 \pm 0.20$, $n = 6$; $b_{\text{TEP-Totalarea}} = -0.18 \pm 0.07$, $r^2 = 0.87 \pm 0.19$, $n = 5$),
11 except for TEP area on day 11 and day 15, and CSP area on day 15. In contrast to total area,
12 only 3 out of 7 observations for TEP abundance and 2 out of 7 for CSP abundance were
13 exponentially related to wind speed. Thus, the relationship between abundance of gel particles
14 in the SML and wind speeds could not be well described by an exponential
15 function. Nevertheless, the reduction of gel particles abundance and area indicated a clear
16 removal from the SML with increasing wind speed. Enrichment of gel particles, with $EF > 1.2$,
17 for both abundance and total area were generally found at wind speed $2\text{--}6 \text{ ms}^{-1}$ (Table 2),
18 excluding day 15 on which high CSP enrichment in the SML ($EF^{\text{SAbundance}} = 4.10$ and EF^{STotal}
19 $\text{area} = 3.20$) was observed at wind speed of 18 ms^{-1} . Enrichment for both CSP and TEP was
20 higher for total area than for abundance at low wind speed (Table 2), suggesting selective
21 enrichment of larger gel particles in the SML.

22 3.3 TEP and CSP size distributions related to wind speeds

23 The power law relation fitted the gel particles size distribution ($d_p: 2\text{--}16 \mu\text{m}$) very well for both
24 CSP and TEP under different wind speed conditions (mean of $r^2 = 0.95$) (Fig. 5 and Fig. 6).



1 Overall, no effect of varying wind speeds on the slopes of the whole size spectrum was
2 determined ($p > 0.05$; two-sample *Kolmogorov-Smirnov test*). However, a significant change
3 on TEP and CSP slopes was observed for wind speed $> 8 \text{ ms}^{-1}$ (Fig. 5 and Fig. 6) ($p < 0.05$;
4 two-sample *Kolmogorov-Smirnov test*). The slopes of size distributions for TEP ranged from -
5 2.93 to -1.32 (median of -2.17, $n=17$) at low and moderate wind speeds ($< 8 \text{ ms}^{-1}$) and were
6 significantly higher than those at high speeds ($> 8 \text{ ms}^{-1}$) ranging from -4.05 to -2.48 (median
7 of -3.32, $n=12$) ($p < 0.05$; two-sample *Kolmogorov-Smirnov test*) (Fig. 7), excluding samples
8 in the SML collected from day 15. Moreover, 8 ms^{-1} was identified also as threshold below
9 which an obvious increase of maximal gel particle size in the SML was found except for day
10 15 (Fig. 8). Similar to TEP, the slopes of CSP were significantly smaller at high wind speed
11 ($> 8 \text{ ms}^{-1}$) (-3.78 to -2.53, median of -3.10, $n=12$) than at $< 8 \text{ ms}^{-1}$ (-3.21 to -2.16, median of -
12 2.59, $n=17$), again except for day 15 ($p < 0.05$; two sample-*Kolmogorov-Smirnov test*) (Fig. 7).
13 However, during the second part of the experiment, when a seed culture of *E.huxleyi* was
14 added on day 20, followed by a biogenic SML from a previous experiment on day 21, no
15 significant difference of CSP size distribution was observed between high and low wind
16 speeds ($p=0.06$, two sample-*Kolmogorov-Smirnov test*), and the negative effect of increasing
17 wind on the maximum size for CSP was less obvious (Fig. 8). Compared to CSP, size
18 distribution of TEP was flatter at low and moderate wind speed ($p < 0.05$), and changes of
19 TEP spectral slopes related to wind speed were more pronounced (Fig. 7).

20 **3.4 Bubble effect on gel particles formation in the SML**

21 An effect of bubbling on the enrichment of gel particles in the SML was seen occasionally.
22 CSP were more enriched in the SML after bubbling in terms of abundance in 6 out of 7
23 experiments, albeit the EF's were only slightly above 1.2 (Table 3). In contrast to abundance,



1 enrichments for total area were less pronounced. Although no significant overall effect of
2 bubbling on SML enrichment in gel particles was determined, it should be noted that higher
3 enrichment factors were observed after bubbling for CSP on day 11 and for TEP on day 22
4 and day 24, respectively.

5

6 **4 Discussion**

7 **4.1 TEP and CSP in SML related to wind speed**

8 Driven by the wind, the friction at the water surface generates a shear current and turbulence
9 in the sea surface microlayer and thus the transport of gases and particles across the interface
10 are closely related. The complexity of the transport processes is caused by the wind blowing
11 over the surface, which not only causes a turbulent shear layer but also generates waves that
12 interact with the turbulent shear layer. The observed differences in concentration, enrichment
13 factor and PSD in response to changes in wind speed revealed that wind speed was a factor
14 controlling of gel accumulation in the SML during the Aeolotron experiment. Similar results
15 were observed during previous studies, which showed that TEP and particulate organic matter
16 concentrations in SML were negatively related to wind speed (Liu and Dickhut, 1998; Wurl et
17 al., 2011). Compression and dilatation of the SML due to capillary waves may increase the
18 rate of polymer collision, subsequently facilitating gel aggregation at lower wind speed (3-4
19 ms^{-1}) (Carlson, 1983). In addition, initial advection generated at wind speeds of 2-3 ms^{-1} ,
20 maintain or enhance enrichments by increasing fluxes of potential microlayer materials to
21 surfaces (Van Vleet and Williams, 1983). As wind speed increases further (4-6 ms^{-1}), wave
22 breaking is likely to increase the turbulence in the top surface layer, but does not cause
23 homogenous mixing (Melville, 1996). This could lead to a reduced gel abundance in the SML,
24 but gel particle remain enrichment in the SML. For higher wind speeds of 8 ms^{-1} and above,



1 the release of momentum from the wave breaking enhances the shear production of energy
2 and further increase the turbulence strength (Donelan, 2013). This could result in more break-
3 up of gel aggregates.

4 Selective loss of larger gels in SML was observed at high wind speed during the Aeolotron
5 experiment, suggesting stronger wind induced shear forces on larger gel particles in the SML.
6 This is because larger particles offer a greater surface area on which the stress of the fluid
7 shear is exerted (Spicer and Pratsinis, 1996; Zhang and Li, 2003). Large gels aggregates may
8 be weaker than smaller as porosity increases with size, and therefore the proportion of
9 constituent matter keeping the aggregate bound together decreases. Similar results were
10 achieved during previous empirical studies and numerical simulations of particle size
11 distribution (PSD) in marine waters, which demonstrated that aggregate breakage has
12 virtually no effect on the size distribution of small particles; instead strong shear of fluid may
13 selectively change the PSD for larger and fractal particles (Beauvais et al., 2006; Li et al.,
14 2004). When fractal scaling is incorporated for colloidal or solid particle characterization,
15 three linear regions with different slopes can also be identified in the size distribution, in
16 accordance with the three collision mechanisms, Brownian motion, fluid shear and
17 differential sedimentation (Kepkay, 1994). The process of collision of particle in shear is
18 typically important for particles larger than a few μm in diameter (Johnson and Kepkay, 1992;
19 Mccave, 1984; O'Melia and Tiller, 1993) and less important than Brownian motion for
20 particles in the submicron size range. It has been suggested that TEP can be formed
21 abiotically by coagulation of colloidal precursors with power law of gel particles size
22 distribution (Alldredge et al., 1993; Jiang and Logan, 1991). Slopes of the TEP size
23 distribution ranging from 2 to 16 μm in SML were in accordance with PSD slopes found
24 when fluid shear is dominant (Li et al., 2004). Also, wind speeds of 8 ms^{-1} significantly
25 changed the PSD of TEP in size range of 2 to 16 μm , corresponding to the presence of wave



1 break and enhanced turbulence. Our observations suggest that PSD of TEP depends on shear
2 induced by wind and wave rather than Brownian motion or differential sedimentation.
3 Furthermore, the exponential decrease of total TEP area in the SML with increasing wind
4 speed may be related to the rate of turbulent kinetic energy dissipation ε ($\text{cm}^2 \text{s}^{-3}$). The
5 relationship between gel concentration and turbulence has been reported to be of an
6 exponential form: $e^{(\varepsilon/2)}$ (Ruiz and Izquierdo, 1997). Therefore, increasing kinetic energy
7 dissipation, which is a linear combination of wind speed, wave and buoyancy forcing within
8 the mixed layer (Belcher et al., 2012), likely induces an exponential decrease in the total area
9 of gels in the SML. However, the exponential relationship was not observed between
10 abundance of gel particle and wind speed in this study, and no significant effect of wind speed
11 on PSD slopes was observed when including small gel particle (dp : 0.4-2 μm) into the
12 analysis. A likely explanation is that the abundance of gel particle was influenced not only by
13 turbulence levels, but also by bubble scavenging and bursting at higher speed. Particularly
14 smaller particles (submicron-micron size range), which contribute more to total gel abundance
15 rather than to total gel area, can accumulate in the SML due to bubble scavenging at high
16 wind speed. This may explain why changes in gel particles abundance did not fit well to an
17 exponential function with wind speed in our study.

18 It has also been suggested that CSP are less prone to aggregation than TEP (Engel and
19 Galgani, 2016; Prieto et al., 2002). During the Aeolotron experiment, the influence of wind
20 speed on spectral slopes was more pronounced for TEP than for CSP. In addition, size
21 distribution of CSP was not affected by wind speed, after adding the *E.huxleyi* seed culture.
22 Our results therefore support the idea that TEP are more prone to aggregation than CSP, and
23 potentially enhance the particle export of out of SML. Nevertheless, appearance of larger CSP
24 in the SML at low wind speed ($<8 \text{ms}^{-1}$) indicate that CSP are also involved in the formation
25 of surface slicks that becomes disrupted when wind speed increases.



1 **4.2 Bubble effect on the enrichment of TEP and CSP**

2 Prior studies have emphasized the importance of air bubbles for physical and biogeochemical
3 processes in the ocean upper layer (Kuhnenn-Dauben et al., 2008; Thorpe et al., 1992). A
4 high gel particles load in the SML may be linked to upward transport by positive buoyant gel
5 particles (Azetsu-Scott and Passow, 2004), or to transport by rising bubbles (Wurl et al.,
6 2009). During this study, CSP and TEP abundance in the SML was more often enriched under
7 bubbling conditions than without bubbles. Proteins are known specifically for their surface
8 activity due to aliphatic groups rendering them intrinsic amphiphiles (Graham and Phillips,
9 1979). As a consequence proteins play a major role in the formation and stabilization of
10 bubbles (Dickinson, 2003). This may explain that CSP were more enriched in the SML after
11 bubbling during this study. Polysaccharide can interlink with protein by covalent bonding or
12 associate via physical interactions (e.g. by electrostatic and hydrophobic interactions, steric
13 exclusion, hydrogen bonding) and affect the interfacial characteristics of the fluid (Patino and
14 Pilosof, 2011). Sulphated polysaccharides interact with charged groups in a protein more
15 strongly than carboxylated hydrocolloids at pH above the protein isoelectric point (Dickinson,
16 2003). Therefore sulphated polysaccharides may be trapped by bubble-films also including
17 proteins (Mopper et al., 1995; Zhou et al., 1998), potentially leading to a higher enrichment of
18 sulfate half-ester groups in the TEP in the SML (Wurl and Holmes, 2008). Depending on the
19 hydrophobicity, different polysaccharide monomeric composition showed either competitive
20 or a cooperative behaviour with proteins (Baeza et al., 2005). Therefore, bubble enhancement
21 likely depends on the composition and proportion of polysaccharides and proteins within gel
22 particle during this study. Moreover, biological factors might affect bubble enhancement of
23 gel particles, i.e. on day 11, the SML was characterized by a strong enrichment of bacteria,
24 and on day 22 and day 24 autotrophic biomass increased (Engel, et al, 2017), corresponding
25 to the higher $EF_{SCSP}^{abundance}$ on day 11 and $EF_{STEP}^{abundance}$ on day 22 and day 24, respectively,



1 under bubbling conditions. This observation is in accordance with findings by Zhou et al.
2 (1998) who showed that TEP formation induced by bubble was related to biological activity.
3 In addition, bubble size (Gantt et al., 2011; Oppo et al., 1999) is also an important factor
4 potentially determining the entrainment of organic matter in the SML. During the Aeolotron
5 experiment, an aerator was used to simulate strong breaking waves for bubble entrainment
6 and spray formation. Unfortunately, the bubble size distribution was not determined. However,
7 under bubbling, the enrichment factors were higher for gel abundance than for total gel area,
8 indicating an increasing amount of smaller size gel particles (a few microns) in the SML. This
9 result is consistent with observations from the high Arctic, which showed that short-chained
10 oligosaccharides might represent an important pool for the formation of small size particles
11 (microcolloids/particles) through bubbling (Gao et al., 2012).

12 **4.3 Implication of biogenic microgels in the SML**

13 In this study, values for $EF_{\text{total area}}$ of gel particles were higher than $EF_{\text{abundance}}$ at lower wind
14 speed. This suggests that large gel particles became selectively enriched in the SML and, due
15 to their larger surface area, may act as a cover sheet, potentially impacting processes across
16 the air-sea interface at low wind speeds. Based on the data of Aeolotron experiment, a
17 schematic diagram on interactions between physical dynamics and gel particle coverage in the
18 SML is proposed (Fig. 9). During this study, the enrichment of TEP and CSP in the SML
19 existed until wind speed reached 6 ms^{-1} , with strong enrichment at about $2\text{--}4 \text{ ms}^{-1}$, at which
20 slick streaks and bands were observed visually. Although surface tension measurements were
21 not made, values for the mean square slope, a measurement of surface roughness, were two or
22 three orders of magnitude higher at wind speeds $> 6 \text{ ms}^{-1}$ than at wind speeds $< 6 \text{ ms}^{-1}$ (Bopp
23 et al., 2017). The large total area of gel particle in the film may have contributed to the
24 observed reductions of wave slope, which would also imply corresponding reductions in mass



1 and momentum exchange at low and mediate wind speed (Frew et al., 2004). At wind speed
2 of 8 ms^{-1} the sea surface became rougher, and micro-wave breaking started. In consequence,
3 the SML started to mix with the subsurface water leading to a more homogeneous distribution
4 of matter in the surface water column; thus a potential role of gel particles in gas-exchange
5 would be reduced. However, under conditions of high wind and wave breaking, microgel
6 precursors and nanogels can be aerosolized with sea spray (Gantt et al., 2011). For the ocean,
7 gel particle emission in aerosols has recently been discussed with respect to cloud formation,
8 precipitation, the hydrological cycle, and climate (Alpert et al., 2011; Knopf et al., 2011;
9 Wilson et al., 2015).

10

11 **5 Conclusion**

12 Our study showed that strong enrichment of biogenic gel particles in SML can occur at low
13 speed ($< 6 \text{ ms}^{-1}$) despite low autotrophic productivity in the water column. A negative
14 exponential relationship between the total area of gel particles in the SML and wind speed
15 was observed in most cases. Our results showed that the PSD slope is an important parameter
16 for characterizing the shape of the gel particle size distribution in the SML and reflects the
17 particles' fate in the SML (i.e. aggregation, fragmentation, sinking and injecting into air).
18 During the Aeolotron experiment, slopes of the TEP size distribution ranging from 2 to $16 \mu\text{m}$
19 in the SML were in accordance with PSD slopes of solid particles previously observed when
20 fluid shear is dominant. Moreover, the slope of PSD for $\text{TEP}_{(2-16\mu\text{m})}$ and the maximum size of
21 gel particles varied significantly at about 8 ms^{-1} . Particle dynamics of TEP and CSP behaved
22 slightly differently. TEP appeared to be more prone to aggregation, potentially enhancing the
23 removal of particle out of SML. Responses of CSP enrichment to bubbling suggested that
24 proteinaceous particles are likely to be preferentially scavenged from the water column and



1 transported upward by bubbles. Overall, variations of gel particles sizes in the SML can
2 provide useful information on particle dynamics at the interface between air and sea.

3 To better understand the role of biogenic gel particles on biophysicochemical processes across
4 the air-sea interface, future studies should consider the full size spectrum of gels scaling from
5 nanometers to micrometers and also include their chemical composition. This could provide
6 important information on implications of marine gels for the aerosol and cloud formation as
7 well as for air-sea gas exchange.

8

9 **Data availability**

10 All data will become available at <https://doi.pangaea.de/upon> publication.

11

12

13

14 **Competing interest**

15 The authors declare that they have no conflict of interest.

16

17 **Acknowledgements**

18 We thank Tania Klüver, Ruth Flerus, Katja Laß, Sonja Endres and Jon Roa for technical
19 assistance. Armin Form helped to collect seawater for the Aeolotron experiment on board of
20 the *RV Poseidon*. This study was supported by the SOPRANIII project (03F06622.2) and by
21 China Scholarship Council (grant number 201408440016). We also thank Bernd Jähne,
22 Kerstin Krall and Maximilian Boppf for providing access and support during the Aeolotron
23 experiment, and for sharing their data and knowledge. This study is a contribution to the
24 international Surface Ocean Lower Atmosphere Study (SOLAS).

25



1

2 **References**

- 3 Allredge, A. L., Passow, U., and Logan, B. E.: The Abundance and Significance of a Class
4 of Large, Transparent Organic Particles in the Ocean, *Deep-Sea Res Pt I*, 40, 1131-1140,
5 1993.
- 6 Alpert, P. A., Aller, J. Y., and Knopf, D. A.: Initiation of the ice phase by marine biogenic
7 surfaces in supersaturated gas and supercooled aqueous phases, *Phys Chem Chem Phys*, 13,
8 19882-19894, 2011.
- 9 Azetsu-Scott, K. and Passow, U.: Ascending marine particles: Significance of transparent
10 exopolymer particles (TEP) in the upper ocean, *Limnol Oceanogr*, 49, 741-748, 2004.
- 11 Baeza, R., Carrera Sanchez, C., Pilosof, A. M. R., and Rodríguez Patino, J. M.: Interactions of
12 polysaccharides with β -lactoglobulin adsorbed films at the air–water interface, *Food*
13 *Hydrocolloids*, 19, 239-248, 2005.
- 14 Beauvais, S., Pedrotti, M. L., Egge, J., Iversen, K., and Marrase, C.: Effects of turbulence on
15 TEP dynamics under contrasting nutrient conditions: implications for aggregation and
16 sedimentation processes (vol 323, pg 47, 2006), *Mar Ecol Prog Ser*, 324, 309-309, 2006.
- 17 Belcher, S. E., Grant, A. L. M., Hanley, K. E., Fox-Kemper, B., Van Roekel, L., Sullivan, P.
18 P., Large, W. G., Brown, A., Hines, A., Calvert, D., Rutgersson, A., Pettersson, H., Bidlot, J.
19 R., Janssen, P. A. E. M., and Polton, J. A.: A global perspective on Langmuir turbulence in
20 the ocean surface boundary layer, *Geophys Res Lett*, 39, 2012.
- 21 Bopp, M. and Jähne, B.: Measurements of the friction velocity in a circular wind-wave tank
22 by the momentum balance method, Unpublished, 2014.
- 23 Bopp, M., Krall, K., and Jähne, B.: Friction velocity and wind wave surface slopes during the
24 SOPRAN Aeolotron Sea- and Freshwater Gas Exchange Experiments, in prep. for *Ocean*
25 *Science*, 2017.
- 26 Calleja, M. L., Duarte, C. M., Prairie, Y. T., Agusti, S., and Herndl, G. J.: Evidence for
27 surface organic matter modulation of air-sea CO₂ gas exchange, *Biogeosciences*, 6, 1105-
28 1114, 2009.
- 29 Carlson, D. J.: Dissolved Organic Materials in Surface Microlayers - Temporal and Spatial
30 Variability and Relation to Sea State, *Limnology and Oceanography*, 28, 415-431, 1983.
- 31 Chow, J. S., Lee, C., and Engel, A.: The influence of extracellular polysaccharides, growth
32 rate, and free coccoliths on the coagulation efficiency of *Emiliana huxleyi*, *Mar. Chem.*, 175,
33 5-17, 2015.
- 34 Cisternas-Novoa, C., Lee, C., and Engel, A.: Transparent exopolymer particles (TEP) and
35 Coomassie stainable particles (CSP): Differences between their origin and vertical
36 distributions in the ocean, *Mar. Chem.*, 175, 56-71, 2015.
- 37 Cunliffe, M., Engel, A., Frka, S., Gasparovic, B., Guitart, C., Murrell, J. C., Salter, M., Stolle,
38 C., Upstill-Goddard, R., and Wurl, O.: Sea surface microlayers: A unified physicochemical
39 and biological perspective of the air-ocean interface, *Prog Oceanogr*, 109, 104-116, 2013.
- 40 Dickinson, E.: Hydrocolloids at interfaces and the influence on the properties of dispersed
41 systems, *Food Hydrocolloid*, 17, 25-39, 2003.



- 1 Donelan, M. A.: Air-Water Exchange Processes. In: Physical Processes in Lakes and Oceans,
2 American Geophysical Union, 2013.
- 3 Engel, A.: Determination of marine gel particles. Practical Guidelines for the Analysis of
4 Seawater, 2009.
- 5 Engel, A.: The role of transparent exopolymer particles (TEP) in the increase in apparent
6 particle stickiness (α) during the decline of a diatom bloom, *J Plankton Res*, 22, 485-497,
7 2000.
- 8 Engel, A., Sperling, M., Sun, C., Grosse, J. and Friedrichs, G.: Bacterial control of organic
9 matter in the surface microlayer: Insights from a wind wave channel experiment. *Limnol.*
10 *Oceanogr.*, submitted.
- 11 Engel, A. and Galgani, L.: The organic sea-surface microlayer in the upwelling region off the
12 coast of Peru and potential implications for air-sea exchange processes, *Biogeosciences*, 13,
13 989-1007, 2016.
- 14 Engel, A. and Galgani, L.: The organic sea surface microlayer in the upwelling region on Peru
15 and implications for air-sea exchange processes, *Biogeosciences Discuss*, 12, 10579-10619,
16 2015.
- 17 Engel, A., Thoms, S., Riebesell, U., Rochelle-Newall, E., and Zondervan, I.: Polysaccharide
18 aggregation as a potential sink of marine dissolved organic carbon, *Nature*, 428, 929-932,
19 2004.
- 20 Falkowska, L.: a field evaluation of teflon plate, glass plate and screen sampling techniques.
21 Part 1. Thickness of microlayer samples and relation to wind speed. In: *Oceanol. Acta*, 1999.
- 22 Frew, N. M., Bock, E. J., Schimpf, U., Hara, T., Haussecker, H., Edson, J. B., McGillis, W.
23 R., Nelson, R. K., McKenna, S. P., Uz, B. M., and Jahne, B.: Air-sea gas transfer: Its
24 dependence on wind stress, small-scale roughness, and surface films, *J Geophys Res-Oceans*,
25 109, 2004.
- 26 Galgani, L. and Engel, A.: Accumulation of Gel Particles in the Sea-Surface Microlayer
27 during an Experimental Study with the Diatom *Thalassiosira weissflogii*., *International*
28 *Journal of Geosciences*, 4, 129-145, 2013.
- 29 Galgani, L., Stolle, C., Endres, S., Schulz, K. G., and Engel, A.: Effects of ocean acidification
30 on the biogenic composition of the sea-surface microlayer: Results from a mesocosm study, *J*
31 *Geophys Res-Oceans*, 119, 7911-7924, 2014.
- 32 Gantt, B., Meskhidze, N., Facchini, M. C., Rinaldi, M., Ceburnis, D., and O'Dowd, C. D.:
33 Wind speed dependent size-resolved parameterization for the organic mass fraction of sea
34 spray aerosol, *Atmos Chem Phys*, 11, 8777-8790, 2011.
- 35 Gao, Q., Leck, C., Rauschenberg, C., and Matrai, P. A.: On the chemical dynamics of
36 extracellular polysaccharides in the high Arctic surface microlayer, *Ocean Sci*, 8, 401-418,
37 2012.
- 38 Garrett, W. D. and Duce, R. A.: Surface Microlayer Samplers. In: *Air-Sea Interaction:*
39 *Instruments and Methods*, Dobson, F., Hasse, L., and Davis, R. (Eds.), Springer US, Boston,
40 MA, 1980.
- 41 GESAMP: The Sea-Surface Microlayer and its Role in Global
42 Change. Reports and Studies, WMO, 1995. 1995.



- 1 Graham, D. E. and Phillips, M. C.: Proteins at liquid interfaces: I. Kinetics of adsorption and
2 surface denaturation, *J Colloid Interf Sci*, 70, 403-414, 1979.
- 3 Jiang, Q. and Logan, B. E.: Fractal Dimensions of Aggregates Determined from Steady-State
4 Size Distributions, *Environ Sci Technol*, 25, 2031-2038, 1991.
- 5 Johnson, B. D. and Kepkay, P. E.: Colloid Transport and Bacterial Utilization of Oceanic
6 Doc, *Deep-Sea Res*, 39, 855-869, 1992.
- 7 Kepkay, P. E.: Particle Aggregation and the Biological Reactivity of Colloids, *Mar Ecol Prog
8 Ser*, 109, 293-304, 1994.
- 9 Knopf, D. A., Alpert, P. A., Wang, B., and Aller, J. Y.: Stimulation of ice nucleation by
10 marine diatoms, *Nature Geoscience*, 4, 88-90, 2011.
- 11 Kuhnenn-Dauben, V., Purdie, D. A., Knispel, U., Voss, H., and Horstmann, U.: Effect of
12 phytoplankton growth on air bubble residence time in seawater, *J Geophys Res-Oceans*, 113,
13 2008.
- 14 Kuznetsova, M., Lee, C., and Aller, J.: Characterization of the proteinaceous matter in marine
15 aerosols, *Mar Chem*, 96, 359-377, 2005.
- 16 Leck, C. and Bigg, E. K.: Source and evolution of the marine aerosol - A new perspective,
17 *Geophys Res Lett*, 32, 2005.
- 18 Li, X. Y., Zhang, J. J., and Lee, J. H. W.: Modelling particle size distribution dynamics in
19 marine waters, *Water Research*, 38, 1305-1317, 2004.
- 20 Liss, P. S. a. D., R. A.: *The Sea Surface and Global Change*, Cambridge University Press,
21 2005.
- 22 Liu, K. W. and Dickhut, R. M.: Effects of wind speed and particulate matter source on surface
23 microlayer characteristics and enrichment of organic matter in southern Chesapeake Bay, *J
24 Geophys Res-Atmos*, 103, 10571-10577, 1998.
- 25 Long, R. A. and Azam, F.: Abundant protein-containing particles in the sea, *Aquat Microb
26 Ecol*, 10, 213-221, 1996.
- 27 Mari, X., Beauvais, S., Lemee, R., and Pedrotti, M. L.: Non-Redfield C : N ratio of
28 transparent exopolymeric particles in the northwestern Mediterranean Sea, *Limnology and
29 Oceanography*, 46, 1831-1836, 2001.
- 30 Mari, X. and Kiorboe, T.: Abundance, size distribution and bacterial colonization of
31 transparent exopolymeric particles (TEP) during spring in the Kattegat, *J Plankton Res*, 18,
32 969-986, 1996.
- 33 Mccave, I. N.: Size Spectra and Aggregation of Suspended Particles in the Deep Ocean,
34 *Deep-Sea Res*, 31, 329-352, 1984.
- 35 Melville, W. K.: The role of surface-wave breaking in the air-sea interaction, *Annu. Rev.
36 Fluid Mech.*, 28, 279-321, 1996.
- 37 Mesarchaki, E., Krauter, C., Krall, K. E., Bopp, M., Helleis, F., Williams, J., and Jahne, B.:
38 Measuring air-sea gas-exchange velocities in a large-scale annular wind-wave tank, *Ocean
39 Sci*, 11, 121-138, 2015.
- 40 Mopper, K., Zhou, J. A., Ramana, K. S., Passow, U., Dam, H. G., and Drapeau, D. T.: The
41 Role of Surface-Active Carbohydrates in the Flocculation of a Diatom Bloom in a Mesocosm,
42 *Deep-Sea Res Pt II*, 42, 47-73, 1995.



- 1 O'Melia, C. R. and Tiller, C. L.: Physicochemical aggregation and deposition in aquatic
2 environments. In: Environmental particles 2 Boca Raton, FL, , Buffle, J. and van, L. H. P.
3 (Eds.), USA, Lewis, 1993.
- 4 Oppo, C., Bellandi, S., Innocenti, N. D., Stortini, A. M., Loglio, G., Schiavuta, E., and Cini,
5 R.: Surfactant components of marine organic matter as agents for biogeochemical
6 fractionation and pollutant transport via marine aerosols, *Mar Chem*, 63, 235-253, 1999.
- 7 Orellana, M. V., Matrai, P. A., Leck, C., Rauschenberg, C. D., Lee, A. M., and Coz, E.:
8 Marine microgels as a source of cloud condensation nuclei in the high Arctic, *P Natl Acad Sci*
9 *USA*, 108, 13612-13617, 2011.
- 10 Passow, U.: Transparent exopolymer particles (TEP) in aquatic environments, *Prog Oceanogr*,
11 55, 287-333, 2002.
- 12 Patino, J. M. R. and Pilosof, A. M. R.: Protein-polysaccharide interactions at fluid interfaces,
13 *Food Hydrocolloid*, 25, 1925-1937, 2011.
- 14 Prieto, L., Ruiz, J., Echevarria, F., Garcia, C. M., Bartual, A., Galvez, J. A., Corzo, A., and
15 Macias, D.: Scales and processes in the aggregation of diatom blooms: high time resolution
16 and wide size range records in a mesocosm study, *Deep-Sea Res Pt I*, 49, 1233-1253, 2002.
- 17 Romano, J. C.: Sea-surface slick occurrence in the open sea (Mediterranean, Red Sea, Indian
18 Ocean) in relation to wind speed, *Deep-Sea Res Pt I*, 43, 411-423, 1996.
- 19 Ruiz, J. E. and Izquierdo, A.: A simple model for the break-up of marine aggregates by
20 turbulent shear, *Oceanologica Acta*, 20, 597-605, 1997.
- 21 Russell, L. M., Hawkins, L. N., Frossard, A. A., Quinn, P. K., and Bates, T. S.: Carbohydrate-
22 like composition of submicron atmospheric particles and their production from ocean bubble
23 bursting, *P Natl Acad Sci USA*, 107, 6652-6657, 2010.
- 24 Spicer, P. T. and Pratsinis, S. E.: Coagulation and fragmentation: Universal steady-state
25 particle-size distribution, *AIChE J.*, 42, 1612-1620, 1996.
- 26 Thorpe, S. A., Bowyer, P., and Woolf, D. K.: Some Factors Affecting the Size Distributions
27 of Oceanic Bubbles, *J Phys Oceanogr*, 22, 382-389, 1992.
- 28 UNESCO: Procedur for sampling the sea surface microlaye. In: *IOC Manuals and Guide 15*,
29 Paris, 1985.
- 30 Van Vleet, E. S. and Williams, P. M.: Surface potential and film pressure measurements in
31 seawater systems I, *Limnol Oceanogr*, 28, 401-414, 1983.
- 32 Wilson, T. W., Ladino, L. A., Alpert, P. A., Breckels, M. N., Brooks, I. M., Browse, J.,
33 Burrows, S. M., Carslaw, K. S., Huffman, J. A., Judd, C., Kilthau, W. P., Mason, R. H.,
34 McFiggans, G., Miller, L. A., Najera, J. J., Polishchuk, E., Rae, S., Schiller, C. L., Si, M.,
35 Temprado, J. V., Whale, T. F., Wong, J. P. S., Wurl, O., Yakobi-Hancock, J. D., Abbatt, J. P.
36 D., Aller, J. Y., Bertram, A. K., Knopf, D. A., and Murray, B. J.: A marine biogenic source of
37 atmospheric ice-nucleating particles, *Nature*, 525, 234+, 2015.
- 38 Wurl, O. and Holmes, M.: The gelatinous nature of the sea-surface microlayer, *Mar Chem*,
39 110, 89-97, 2008.
- 40 Wurl, O., Miller, L., Ruttgers, R., and Vagle, S.: The distribution and fate of surface-active
41 substances in the sea-surface microlayer and water column, *Mar Chem*, 115, 1-9, 2009.



- 1 Wurl, O., Miller, L., and Vagle, S.: Production and fate of transparent exopolymer particles in
- 2 the ocean, *J Geophys Res-Oceans*, 116, 2011.
- 3 Wurl, O., Stolle, C., Van Thuoc, C., The Thu, P., and Mari, X.: Biofilm-like properties of the
- 4 sea surface and predicted effects on air-sea CO₂ exchange, *Prog Oceanogr*, 144, 15-24, 2016.
- 5 Zhang, J.-j. and Li, X.-y.: Modeling particle-size distribution dynamics in a flocculation
- 6 system, *AIChE J.*, 49, 1870-1882, 2003.
- 7 Zhou, J., Mopper, K., and Passow, U.: The role of surface-active carbohydrates in the
- 8 formation of transparent exopolymer particles by bubble adsorption of seawater, *Limnol*
- 9 *Oceanogr*, 43, 1860-1871, 1998.
- 10
- 11
- 12
- 13
- 14
- 15
- 16
- 17
- 18
- 19
- 20
- 21
- 22
- 23
- 24
- 25
- 26
- 27
- 28
- 29
- 30



1 **Table caption**

2

3 Table 1. Wind speed settings on the Aeolotron regular experimental days

4

5 Table 2. The enrichment factor of gel particles abundance and total area at different wind
6 speeds

7

8 Table 3. Enrichment factors of TEP and CSP under Bubble bursting and without Bubbles
9 conditions

10

11

12

13

14

15

16

17

18

19

20

21

22

23

24

25

26



1 Table 1. Wind speed settings during the Aeolotron experimental days. (*) indicates that an
 2 aerator was used to simulate strong breaking waves with bubble entrainment and spray
 3 formation under these wind speeds condition.

Day	Wind velocity U_{10}						
2	NaN	NaN	3.98	5.376	11.068	NaN*	17.892
4	2.092	3.437	4.305	8.306	14.145	13.448*	
9	1.536	2.404	4.072	5.291	11.080	10.218*	
11	1.663	2.89	3.925	8.033	13.955	18.208*	NaN
15	2.580	4.985	6.424	11.095	18.090	17.991*	
22	1.371	1.371	4.529	6.099	11.283	10.294*	18.652
24	1.438	2.645	4.269	5.375	11.369	10.397*	18.130

4

5

6

7

8

9

10

11

12

13

14

15

16

17

18

19

20

21

22



- 1 Table 2. Enrichment factors (EF) for gel particles abundance and total area in the SML at
 2 different wind speeds ($EF_{Total\ area} > EF_{Abundance}$ are marked bold at low wind speeds)

Experiment day	Wind speed ($m\ s^{-1}$)	TEP		CSP	
		$EF_{Abundance}$	$EF_{Total\ area}$	$EF_{Abundance}$	$EF_{Total\ area}$
2	NaN(<4ms⁻¹)	2.24	7.40	41.43	113.98
	17.892	1.80	1.71	8.21	12.27
4	2.092	0.97	5.71	3.52	26.81
9	1.536	3.34	16.16	nd	nd
	2.404	4.80	12.76	1.84	7.08
	5.291	1.44	5.40	1.20	2.78
	11.080	1.08	1.07	0.74	0.72
11	3.925	0.91	1.16	13.46	31.16
	18.208	1.63	1.53	1.11	1.12
15	2.580	1.06	1.13	1.28	1.03
	4.985	0.48	0.77	0.47	1.08
	6.424	0.68	0.95	1.39	2.02
	11.095	0.77	0.70	2.14	1.50
	18.090	1.28	1.02	4.10	3.20
22	1.371	3.06	4.38	1.14	2.41
	4.529	3.06	5.04	5.46	4.54
	6.099	2.94	4.78	1.34	2.23
	11.283	0.61	1.02	1.07	1.02
	18.652	0.44	0.58	1.41	0.85
24	1.438	4.68	8.21	1.82	3.93
	4.269	6.97	6.06	5.94	6.82
	5.375	6.42	5.19	2.44	4.05
	11.369	2.38	1.23	0.72	0.66
	18.130	1.74	0.81	0.65	0.69

3

4

5

6

7

8

9

10

11

12



1 Table 3. Enrichment factors (EF) of TEP and CSP in the SML with and without bubbling of
2 the water column in the Aeolotron.

Experiment day	Wind speed (ms ⁻¹)	No bubbles		Bubbles		No bubbles		Bubbles	
		TEP Abund.	TEP Area	TEP Abund.	TEP Area	CSP Abund.	CSP Area	CSP Abund.	CSP Area
4	13.448	nd	nd	3.11	1.91	nd	nd	1.47	1.12
9	10.218	1.08	1.07	1.29	1.24	0.74	0.72	1.70	1.12
11	nd (~18)	1.63	1.53	0.73	0.90	1.11	1.12	2.84	2.63
15	17.991	1.28	1.02	1.09	0.99	4.10	3.20	3.19	1.54
22	10.294	0.61	1.02	1.76	1.37	nd	nd	0.61	0.63
24	10.397	2.38	1.23	4.13	1.06	0.72	0.66	0.95	0.94
5	18.209	0.93	0.76	1.12	1.01	1.15	1.03	1.64	1.09
12	17.983	1.48	1.30	0.56	0.64	0.64	1.07	1.47	1.11
23	17.932	1.33	1.07	1.17	0.65	0.94	1.23	5.44	2.19

3

4

5

6

7

8

9

10

11

12

13

14

15

16

17

18

19



1 **Figure captions**

2 Figure 1: Schematic of wind speed (U_{10}) increase during the experiments conducted in the
3 Aeolotron.

4 Figure 2: Developments of TEP and CSP in the SML and the bulk water in the course of the
5 Aeolotron study.

6 Figure 3: Response of TEP abundance and total area to increasing wind speeds.

7 Figure 4: Response of CSP abundance and total area to increasing wind speeds.

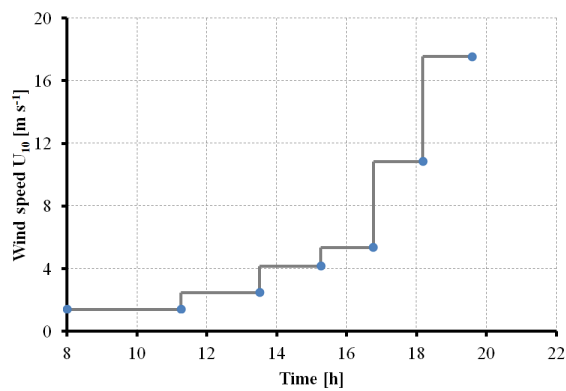
8 Figure 5: PSD of TEP in the SML at different wind speeds. Linear regressions of
9 $\log(dN/d(dp))$ vs. $\log(dp)$ were fitted to particles in the size range of 2-16 μm ESD, with wind
10 speeds $< 8 \text{ ms}^{-1}$ (solid line) and wind speeds $> 8 \text{ ms}^{-1}$ (dash and dot).

11 Figure 6: PSD of CSP in the SML at different wind speeds. Linear regressions of
12 $\log(dN/d(dp))$ vs. $\log(dp)$ were fitted to particles in the size range of 2-16 μm ESD, with wind
13 speeds $< 8 \text{ ms}^{-1}$ (solid line) and wind speeds $> 8 \text{ ms}^{-1}$ (dash and dot).

14 Figure 7: Box chart of slopes (δ) of gel size distribution at low and moderate wind speeds ($<$
15 8 ms^{-1}) and at high wind speeds ($> 8 \text{ ms}^{-1}$) (data for day 15 excluded due to no significant
16 response of PSD to wind speed on day 15)

17 Figure 8,A-D: Maximum size (ESD) of gel particles in the SML; A) and C): before addition
18 of *E.huxleyi*; B) and D): after addition of *E.huxleyi*.

19 Figure 9,A-G: A strong accumulation of TEP and CSP occurred at low wind speed as
20 determined by microscope, A: TEP (2.0 ms^{-1}), B: TEP (4.3 ms^{-1}), C: TEP (8.3 ms^{-1}), D: CSP
21 (2.0 ms^{-1}), E: CSP (4.3 ms^{-1}), F: CSP (8.3 ms^{-1}); G: Proposed schematic for interactions
22 between physical dynamics and gel particle coverage in the SML.



1

2

3

4

5

6

7

8

9

10

11

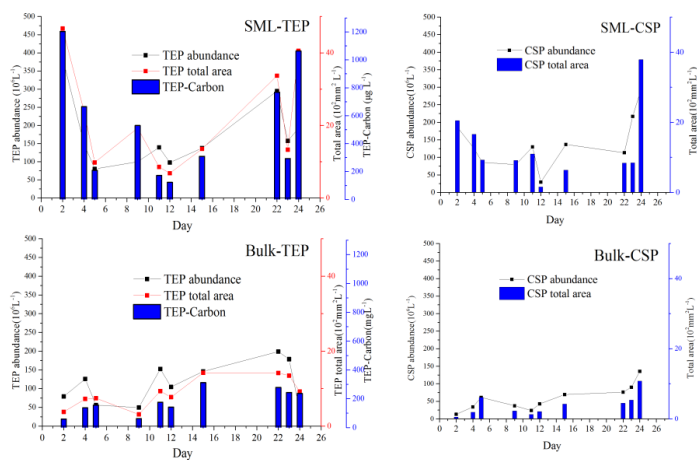
12

13

14

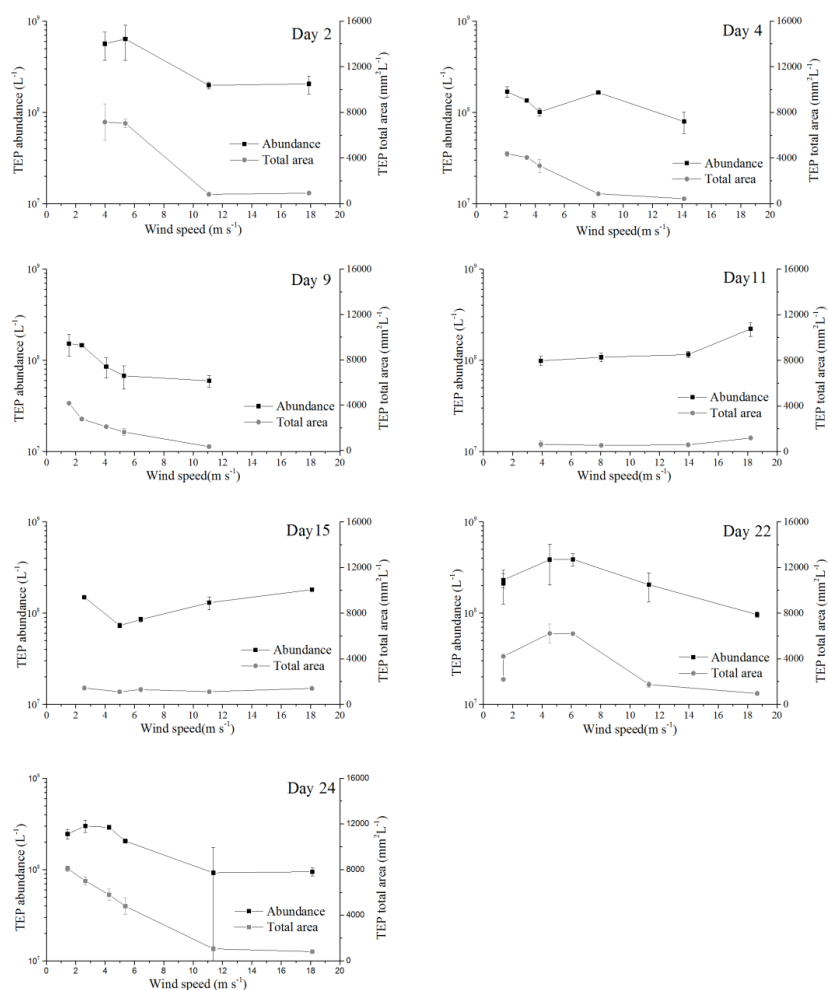
15

Figure 1



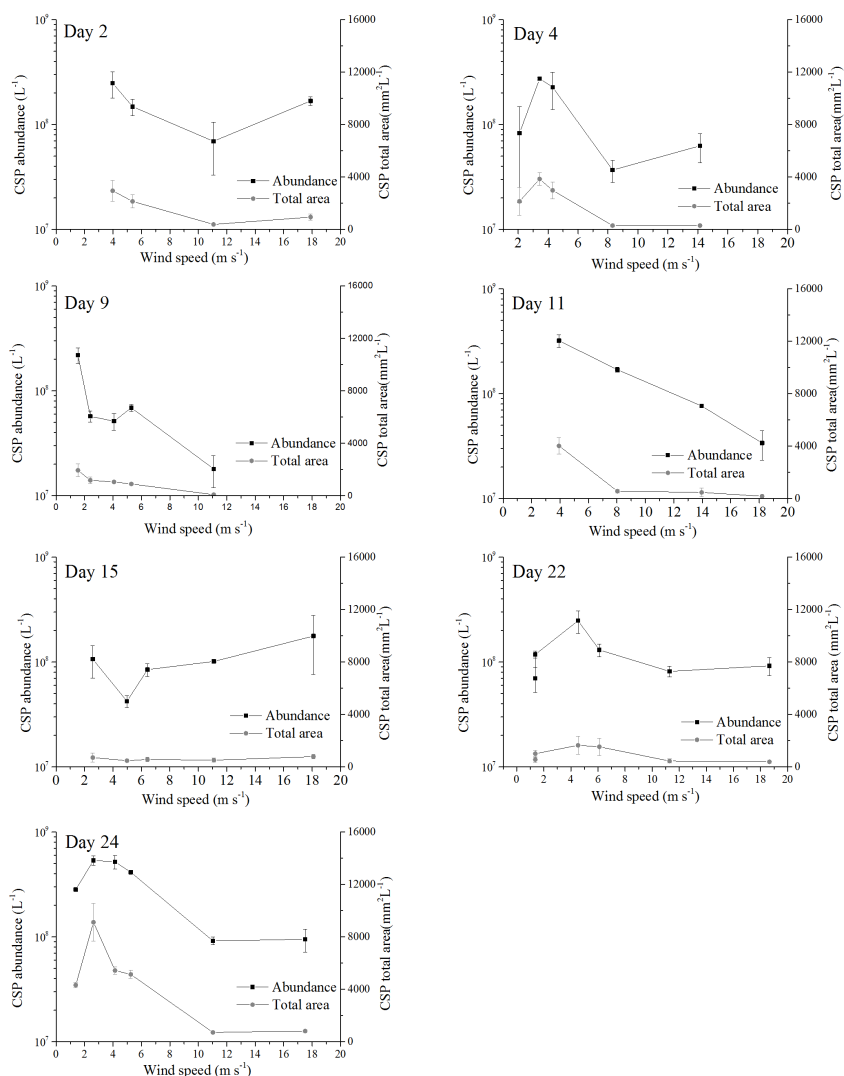
1
2
3
4
5
6
7

Figure 2



1
2
3
4
5
6

Figure 3

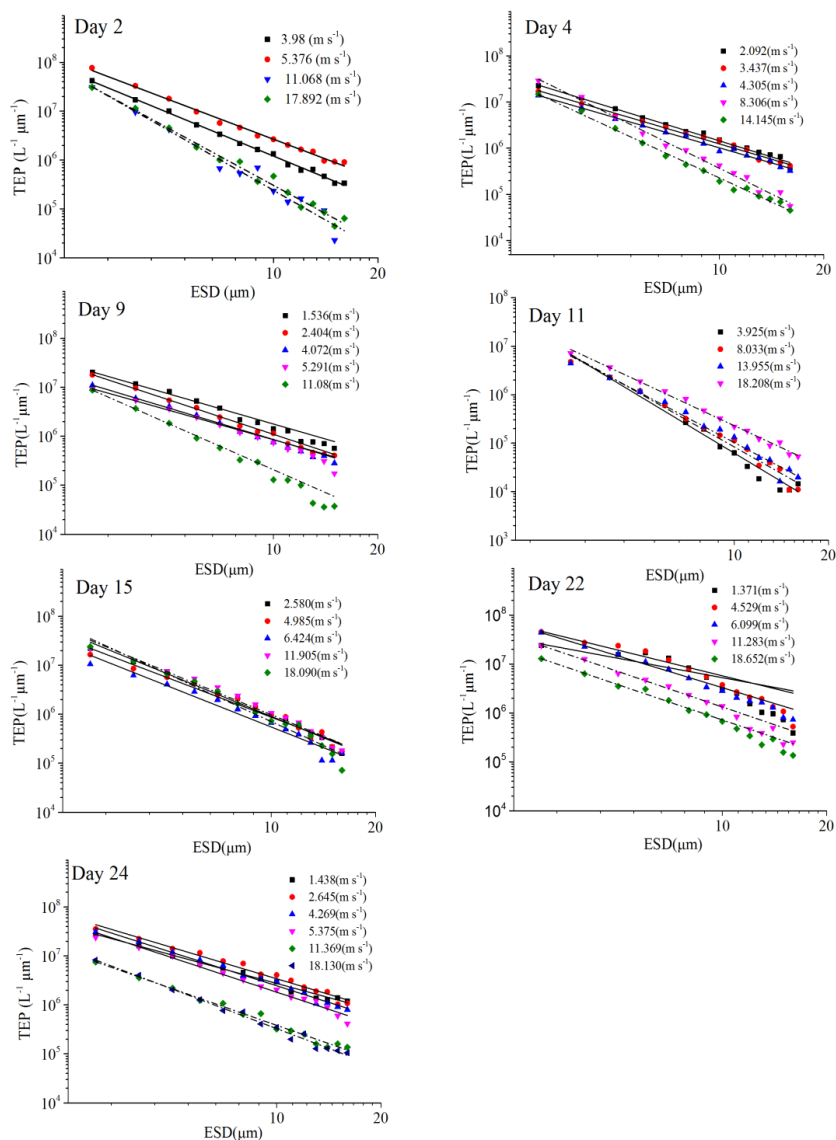


1

2

3

Figure 4



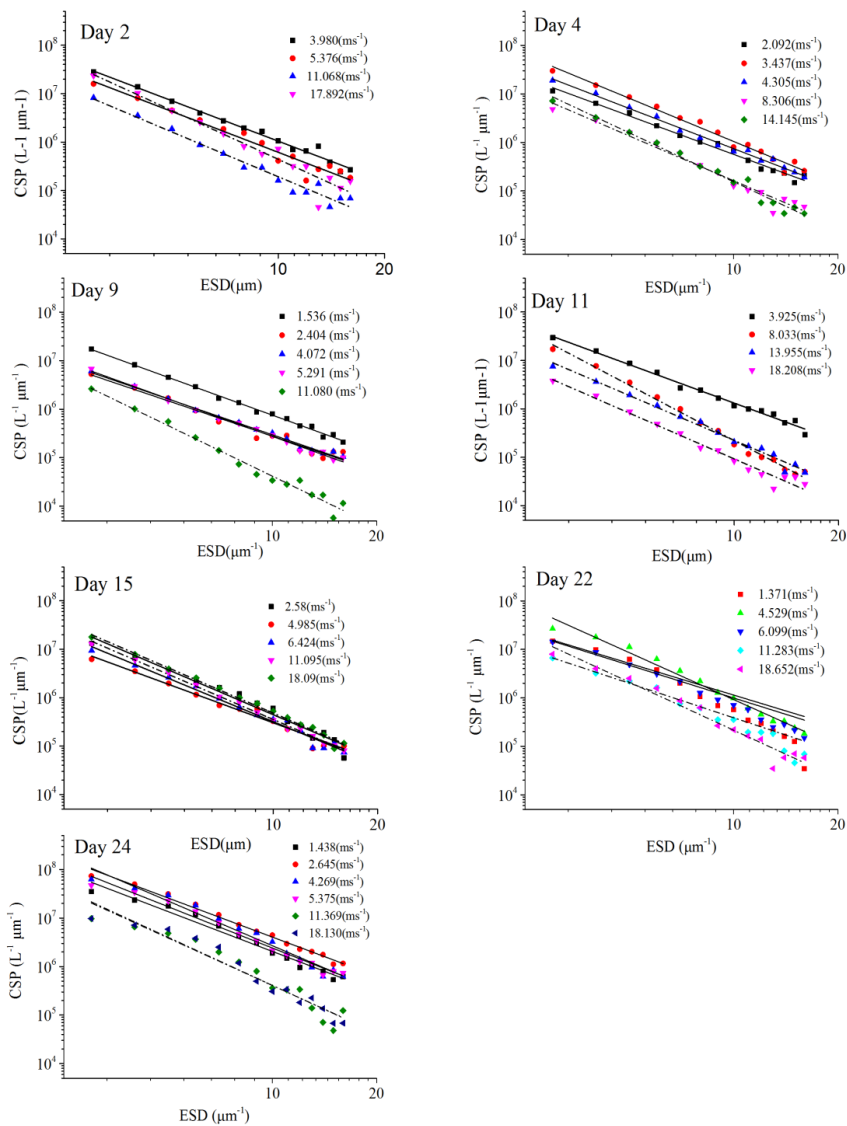
1

2

3

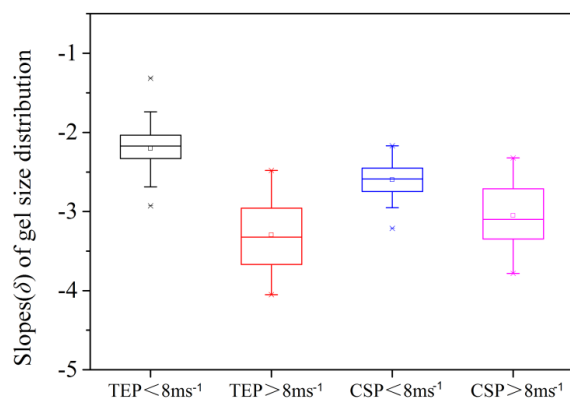
4

Figure 5



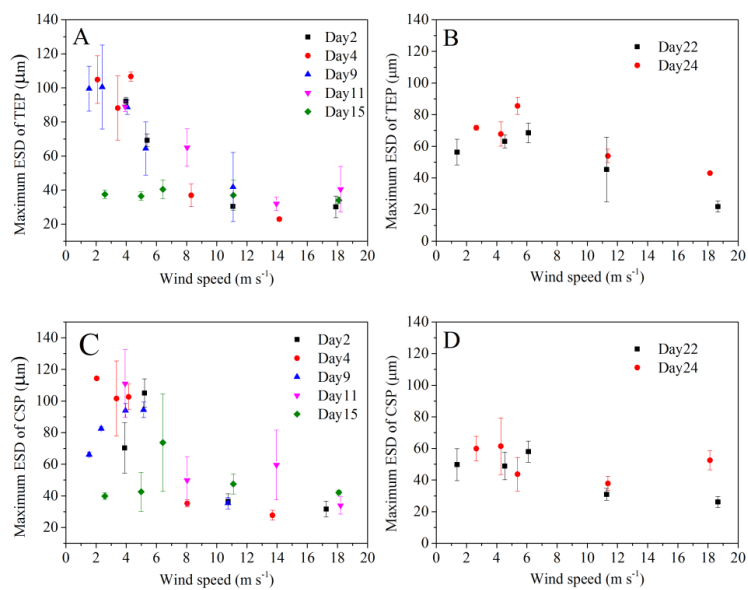
1
2
3
4

Figure 6



1
2
3
4
5
6
7
8
9
10
11
12
13
14
15

Figure 7

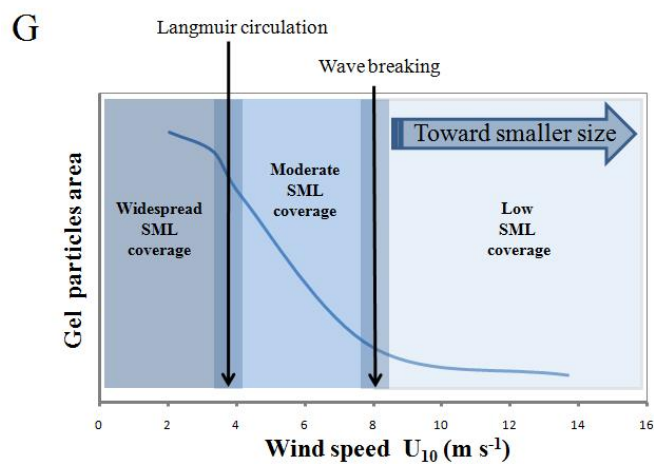
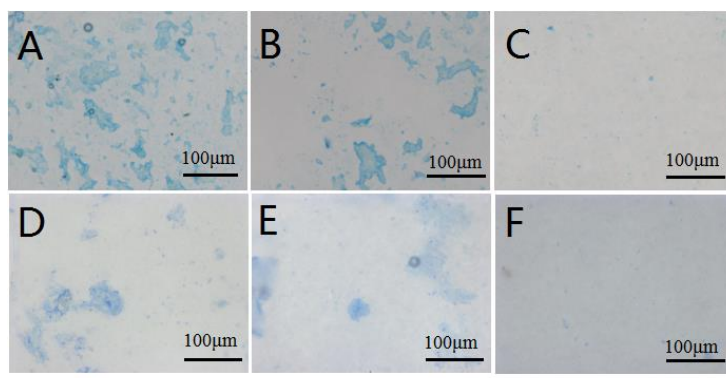


1
2
3
4
5
6
7
8
9
10
11
12
13
14

Figure 8



1



2

3

4

5

6

7

8

9

10

Figure 9